

^1H NMR-based metabolomics approach reveals metabolic alterations in response to dietary imbalances in *Megalobrama amblycephala*

Panita Prathomya¹ · Wassana Prisingkorn¹ · Ivan Jakovlić² · Fang-Yu Deng¹ · Yu-Hua Zhao¹ · Wei-Min Wang¹

Received: 3 October 2016 / Accepted: 21 December 2016 / Published online: 10 January 2017
© Springer Science+Business Media New York 2017

Abstract

Introduction High-fat and high-carbohydrate diets cause a number of metabolic disorders in mammals. However, little is known about metabolomic changes caused by dietary imbalances in fish.

Objectives The objective of this study was to assess the impacts of high-fat diet (HFD), high-carbohydrate diet (HCD) and high-fat-high-carbohydrate diet (HFHCD) on metabolites in a farmed cyprinid fish *Megalobrama amblycephala*.

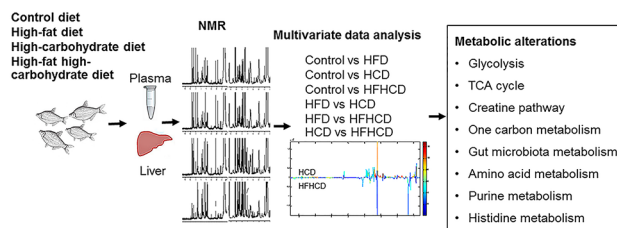
Methods We have employed the ^1H NMR-based metabolomic approach to measure the concentrations of metabolites in plasma and liver of four different diet groups: HFD, HCD, HFHCD and control. Multivariate statistical analyses were used to determine significantly changed metabolites between all group-pairs.

Results All three test diets have affected metabolic profiles, phenotypes and clinical chemistry. High-fat diets

(HFD, HFHCD) resulted in a higher average weight than HCD, but high-carbohydrate diets (HCD, HFHCD) caused signs of liver damage. HCD has resulted in elevated metabolites in energy pathways, leading to further disturbances in creatine pathway. Excess of carbohydrate and lipid metabolism products in the HFHCD group appears to have caused “congestion” of the TCA cycle, causing a significant decline in the numbers of amino acids entering the cycle, which in turn resulted in elevated levels of seven amino acids in this group. Gut microbiota metabolites (TMA) exhibited a strong positive correlation with the carbohydrate content and a negative correlation with the fat content in diets.

Conclusion These results provide an important insight into the diet-affected metabolic disorders that often lead to financial losses in the aquaculture of *Megalobrama amblycephala*.

Graphical Abstract



Electronic supplementary material The online version of this article (doi:10.1007/s11306-016-1158-7) contains supplementary material, which is available to authorized users.

✉ Yu-Hua Zhao
zhaoyuhua2005@mail.hzau.edu.cn

✉ Wei-Min Wang
wangwm@mail.hzau.edu.cn

¹ Key Lab of Freshwater Animal Breeding, Key Lab of Agricultural Animal Genetics, Ministry of Agriculture, Breeding and Reproduction of Ministry of Education, Freshwater Aquaculture Collaborative Innovation Center of Hubei Province, College of Fisheries, Huazhong Agricultural University, Wuhan 430070, People's Republic of China

² Bio-Transduction Lab, Wuhan Institute of Biotechnology, Wuhan 430075, People's Republic of China

Keywords High-fat diet · High-carbohydrate diet · Metabolic pathway · Metabolite · Wuchang bream · Fish

1 Introduction

Oxidation of carbohydrates and triglycerides provides the energy for metabolic activities of cells in animal organisms. Their metabolic pathways are highly interconnected, mostly by converging at the TCA cycle, but also via a large number of precursors and byproducts. High-fat and high-carbohydrate diets cause increased levels of hepatic lipogenesis (Koteish and Diehl 2001), and hence are an important component of the etiology of obesity and hepatic steatosis (Asai et al. 2014).

Megalobrama amblycephala is a predominantly herbivorous cyprinid fish native to China, with a fast-growing yearly output that currently places it among the top seven species in the Chinese aquaculture production (Food and Agriculture Organization of the United Nations 2013). The aquaculture of this species has also been affected by the global trend in aquatic animal feed production to use high levels of carbohydrates and fat in order to reduce the amount of costly protein in the feed (Gao et al. 2009; Li et al. 2013, 2014; Ren et al. 2015; Wang et al. 2015). This often causes a number of metabolic disorders, such as hepatic steatosis and weakened immune responses, resulting in high mortality and lower market value of the farmed fish (Li et al. 2012, 2013; Zhou et al. 2013).

As the products of carbohydrate and fat metabolisms are moved by blood through the body, the effects of imbalanced diets and associated metabolic disorders can be assessed by measuring the concentrations of their by-products in blood (Figueiredo-Silva et al. 2012; Ge et al. 2016; Horton et al. 1995; Polakof et al. 2011; Yamashita et al. 2001). Nutritional metabolomics studies provide a mechanism to use biochemical pathways to study the impact of diet on the incidence of metabolic disorders and diseases (An et al. 2013; Duan et al. 2013; Jiang et al. 2013; Jung et al. 2012; Kim et al. 2010). Metabolomics can be employed to investigate the metabolic changes in a holistic manner (systems biology) (Dunn et al. 2011), as well as in specific organs (Ong et al. 2009). Even though metabolomics has been widely applied in nutritional studies in fish (Akhtar et al. 2016; Kullgren et al. 2010; Schock et al. 2012; Zhao et al. 2014), metabolomic approach has not yet been used to study the impacts of diet on obesity and hepatic steatosis in fish. Hence, the impacts of the excess of the two main energy-providing diet components, carbohydrates and fat, on the fish metabolome remain poorly understood. The excess of these might result in imbalances in the central cellular energy pathway, which might be also reflected on a number of related metabolic pathways that share precursors with it. Hence, in order to better understand the diet-induced metabolic disorders that often plague the aquaculture of *M. amblycephala*, we have undertaken a comparative metabolomic analysis of plasma and liver of

fish fed four different diets: control, high-fat diet (HFD), high-carbohydrate diet (HCD), and high-fat-high-carbohydrate diet (HFHCD). To be able to assess the footprint of each diet on the metabolic profile, we have compared the three experimental diets to the control diet. Furthermore, as carbohydrates and triglycerides could exhibit unique interactions in metabolic pathways, we have also compared the metabolic profiles among the three experimental diets: HFD versus HCD, HFD versus HFHCD, and HCD versus HFHCD. Once we have identified the significantly changed metabolites between group-pairs, categorization of these altered metabolites into metabolic pathways will lead to a better understanding of the connection between diet and metabolic disorders in *M. amblycephala*.

2 Materials and methods

2.1 Chemicals

Analytical grade sodium chloride, $\text{NaH}_2\text{PO}_4 \cdot 2\text{H}_2\text{O}$, and $\text{K}_2\text{HPO}_4 \cdot 3\text{H}_2\text{O}$ were purchased from Sinopharm Chemical Reagent Co. Ltd. (Shanghai, China); deuterium oxide (D_2O , 99.9% D) and sodium 3-trimethylsilyl [2,2,3,3- $^2\text{H}_4$]-propionate (TSP) from Sigma-Aldrich Inc. (USA); and sodium azide (NaN_3) from Tianjin Fu Chen Chemicals Reagent Factory (China). NMR tubes were purchased from NORELL, Inc. (Marion, USA).

2.2 Experimental fish, diets and sample collection

Juvenile *M. amblycephala* were obtained from the Huazhong Agricultural University (Wuhan, China) fish breeding base. The fish were placed in a fiberglass tank and fed a commercial feed during the acclimation period (14 days), at the end of which they were randomly divided into 12 tanks ($n=45$). Three tanks ($n=135$) were randomly assigned to each diet group (3 replicates \times 4 diet-groups): control (C; containing 8.0% fat and 26.7% carbohydrates), high fat diet (HFD; containing 12.2% fat and 27.8% carbohydrates), high carbohydrate diet (HCD; containing 8.3% fat and 34.1% carbohydrates) and high fat high carbohydrate diet (HFHCD; containing 10.4% fat and 30.9% carbohydrates) (Table S2). Water temperature was controlled (25 ± 0.5 C°). The fish (average weight at the beginning of the experiment = 48.13 ± 0.27 g) were fed by hand to satiation twice daily for 56 days. The amount of food intake and uneaten feed were recorded and collected daily. At the end of the experiment, after a 12-hour fast, the fish were anesthetized, weighed, and sacrificed. Fifteen specimens per each group were selected randomly to collect blood and liver samples. Ten blood and liver samples were randomly selected for clinical

chemistry measurements, histopathological examinations and metabolomics analysis, and five samples were kept as reserve. Blood samples ($n=10$) were obtained following the standard protocol, using sodium heparin as anticoagulant. Each sample was divided into two tubes: for clinical chemistry measurements and metabolomics analysis. All blood samples were centrifuged immediately after collection and supernatant stored at -80°C . Liver tissue samples ($n=10$) were weighed and each individual sample divided into two tubes: one to be fixed in 10% formalin for histopathological examination, and the other one to be immediately flash-frozen with liquid nitrogen and stored at -80°C until used for metabolomics analysis.

2.3 Clinical chemistry analysis and histopathological assessment

Serum biochemistry parameters were examined for lipid content and liver damage diagnostic (Li et al. 2012) with commercial kits produced by Jiancheng Bioengineering Institute (Nanjing, China) using a TECAN analyzer. The measured serum parameters included alanine aminotransferase (ALT), aspartate aminotransferase (AST), triglycerides (TG), low-density lipoprotein (LDL) cholesterol, high-density lipoprotein (HDL) cholesterol, and total cholesterol (tChol). Formalin-fixed liver tissues were embedded in paraffin wax, sectioned (3–4 μm), and stained using the hematoxylin and eosin method to assess the damage and fat droplet accumulation in liver. Microscopic assessment was carried out by a qualified pathologist.

2.4 Preparation of plasma and liver samples for the NMR analysis

Each plasma sample (170 μL) was mixed with 340 μL phosphate buffer (45 mM, pH 7.47, 50% D_2O) containing 0.9% NaCl in a 5 mm NMR tube and used directly for the NMR analysis. Liver tissues (about 50 mg) were homogenized in cold methanol and water ($v/v=2:1$) using a Qiagen Tissue-Lyser (Retsch GmbH, Germany). The supernatant (550 μL) was collected after centrifugation (16 099 g, 4°C , 10 min). The extraction was repeated thrice using the same procedure. The supernatants collected from the above procedure were mixed together and freeze-dried after the removal of methanol in vacuo. Then the residue was dissolved in 600 μL of phosphate buffer (0.15 M, pH 7.38, 80% D_2O) containing 0.001% TSP and 0.01% NaN_3 . The supernatant (550 μL) was transferred into a 5 mm NMR tube.

2.5 NMR spectroscopic analysis

All plasma NMR spectra were acquired at 298 K on a Bruker AVance III 600 MHz NMR spectrometer (600.13 MHz for ^1H frequency) equipped with a cryogenic probe (Bruker Biospin, Germany). 1D ^1H NMR spectra were acquired using the Carr-Purcell-Meiboom-Gill (CPMG) pulse sequence ($\text{RD-}90^{\circ}\text{-(}\tau\text{-}180^{\circ}\text{-}\tau\text{)}_n\text{-ACQ}$), where $\tau=350$ ms and $n=100$. For liver extract samples, we used the first increment of the NOESY pulse sequence ($\text{RD-}90^{\circ}\text{-}t_1\text{-}90^{\circ}\text{-}t_m\text{-}90^{\circ}\text{-acquisition}$; $t_1=4$ μs , $t_m=100$ ms). A total of 64 transients for all samples were collected into 32 K data points over a spectral width of 20 ppm with 90° pulse length adjusted to about 10 ms.

For resonance assignment purpose, a series of two-dimensional (2D) NMR spectra were acquired and processed as previously described (Dai et al. 2010a, b). These included ^1H - ^1H correlation spectroscopy (COSY), ^1H - ^1H total correlation spectroscopy (TOCSY), ^1H J-resolved spectroscopy (JRES), ^1H ^{13}C heteronuclear single-quantum correlation spectroscopy (HSQC), and ^1H - ^{13}C heteronuclear multiple bond correlation (HMBC) 2D NMR spectra (Supplementary data Fig. S2).

2.6 NMR spectral data analysis

The free induction decays were multiplied by an exponential window function with the line-broadening factor of 1 Hz prior to Fourier Transformation. Each spectrum was corrected for phase and baseline deformation manually using Topspin 2.1 (Bruker Biospin) and the chemical shift of alpha-glucose was calibrated at δ 5.23. The spectral region between δ 0.5–8.5 was integrated into bins with a width of 0.004 ppm using AMIX v3.9.2 package (Bruker Biospin). Some unwanted signals, such as water (δ 4.55–5.15) and urea resonance (δ 5.56–5.96), were removed. The areas of all bins were then normalized to the probabilistic quotient. Multivariate statistical analysis was undertaken as described in Qiu et al. (2016). The models were constructed using the partial least square discriminant (PLS-DA) and orthogonal projection to the latent structure-discriminant analysis (OPLS-DA) with Unit Variance (UV) scaling, and validated with a seven-fold cross-validation method using SIMCA-P1 v 12.0 (Umetrics, Sweden). The significance of the OPLSDA model was also validated by CV-ANOVA. Differences were considered statistically significant at the $p<0.05$ level. Metabolites exhibiting significantly different concentrations in different group-pairs were visualized in score plots. To assist the biological interpretation of the loadings generated from the model, the loadings were first back-transformed and then plotted with colour-coded OPLS-DA coefficients in MATLAB 7.1. The colour code corresponds to the absolute value of the

OPLS-DA correlation coefficient $|r|$, which indicates the contribution of the corresponding variable to the group separation. In these loadings plots, hot-colored (the red end of the spectrum) metabolites contributed more significantly to the intergroup differences than cold-colored (blue) ones. The cutoff value ($|r| > 0.602$) used in this study was based on the discrimination significance value ($p < 0.05$), which was determined according to the test for significance of the Pearson's product-moment correlation coefficient ($n = 10$, $p < 0.05$). Kyoto Encyclopedia of Genes and Genomes database (KEGG) was used to associate metabolites with metabolic pathways. To evaluate the validity of the PLS-DA models, a permutation test ($n = 200$) was used. Meanwhile, the R^2 value and the difference between R^2 and Q^2 were used to evaluate the possibility of over-fit models (Qiu et al. 2016).

3 Results and discussion

We have studied the impacts of four different diets on metabolomic profiles of plasma and liver of juvenile *Megalobrama amblycephala*. The significantly impacted metabolites were associated with several metabolic pathways, including glycolysis, TCA cycle, gut microbiota metabolism, purine metabolism, histidine metabolism, one carbon metabolism and amino acids metabolism.

3.1 Phenotypes and clinical chemistry of the experimental fish

The three imbalanced diets induced metabolic changes that affected the phenotypes and clinical chemistry of the experimental fish (Table 1). High-fat diets (HFD and HFHCD) resulted in higher average final weight, which is in good agreement with studies on mice (Jung et al.

2012) and humans, where overfeeding on fat has resulted in much higher weight gain (90–95%) and lower energy expenditure than overfeeding on carbohydrates (Horton et al. 1995). Hence, the lower weight of the HCD group (which was still higher than the control group), could be a consequence of a higher metabolic rate (in comparison to high-fat diets), induced by high-carbohydrate diet, resulting in higher energy requirements (Horton et al. 1995). However, in comparison to HFD, high-carbohydrate diets (HCD and HFHCD) caused stronger signs of liver damage and higher levels of metabolic disruption. Clinical chemistry results showed that, in comparison to other diets, the HFHC diet resulted in significantly ($p < 0.05$) altered LDL (higher) and HDL (lower) values in serum. This suggests that HFHC diet caused elevated levels of cholesterol synthesis in liver and its subsequent release into blood as HDL and LDL. High levels of LDL are a predictor of several chronic diseases, whereas HDL (so called “good cholesterol”) can reduce LDL levels in blood. AST value was elevated in the HCD group and ALT was elevated in both high-carbohydrate groups (HCD and HFHCD). High ALT and AST levels are an indication of liver damage (Peng et al. 2011), but high AST levels might also be an indication of changes in the TCA cycle and amino acids metabolism (further discussed in Sect. 3.3.1). Interestingly, neither of the two parameters was significantly different between the control and HFD groups. This absence of liver damage markers was also observed in HFD-fed rats (Xie et al. 2010). Histological analyses found that liver cells of fish from the control diet group had large and round nuclei, and exhibited very mild accumulation of small lipid droplets. HFD led to a moderate accumulation of lipid droplets and swelling hepatocytes, with irregular nucleus located at the periphery of the cell. HCD and HFHCD groups exhibited large lipid droplets with swollen hepatocytes and nuclear degeneration (Fig. 1). This is in good agreement with high

Table 1 Phenotypes and plasma biochemical parameters of fish fed control, high-fat (HFD), high-carbohydrate (HCD) and high-fat-high-carbohydrate (HFHCD) diets

Parameters	Treatments			
	Control	HFD	HCD	HFHCD
Initial weight (g)	48.15 ± 0.55 ^a	48.15 ± 0.36 ^a	48.11 ± 0.22 ^a	48.11 ± 0.11 ^a
Final weight (g)	65.28 ± 2.95 ^a	72.74 ± 1.54 ^b	68.53 ± 2.78 ^{ab}	71.63 ± 4.01 ^b
Weight gain (%)	35.56 ± 5.14 ^a	51.07 ± 2.24 ^b	42.42 ± 5.13 ^{ab}	48.90 ± 8.54 ^b
HSI (%)	1.40 ± 0.14 ^b	1.26 ± 0.11 ^a	1.52 ± 0.13 ^c	1.35 ± 0.08 ^{ab}
TG (mmol/L)	0.86 ± 0.19 ^a	0.86 ± 0.25 ^a	0.71 ± 0.16 ^a	0.89 ± 0.22 ^a
TCHOL (mmol/L)	6.98 ± 2.11 ^a	6.77 ± 1.18 ^a	5.62 ± 0.84 ^a	5.79 ± 1.09 ^a
LDL (mmol/L)	1.94 ± 0.95 ^a	2.50 ± 0.67 ^a	2.70 ± 1.25 ^a	3.66 ± 0.97 ^b
HDL (mmol/L)	3.75 ± 1.64 ^a	4.01 ± 0.84 ^b	4.07 ± 0.70 ^b	2.87 ± 0.99 ^a
AST (mmol/L)	35.42 ± 17.21 ^a	36.83 ± 10.67 ^a	44.55 ± 15.53 ^b	36.50 ± 8.89 ^a
ALT (mmol/L)	8.43 ± 5.79 ^a	8.29 ± 5.10 ^a	12.55 ± 7.57 ^b	13.49 ± 8.97 ^b

Values are presented as means ± SD of three replicates. Values within the same row with different superscripts are significantly different ($p < 0.05$)

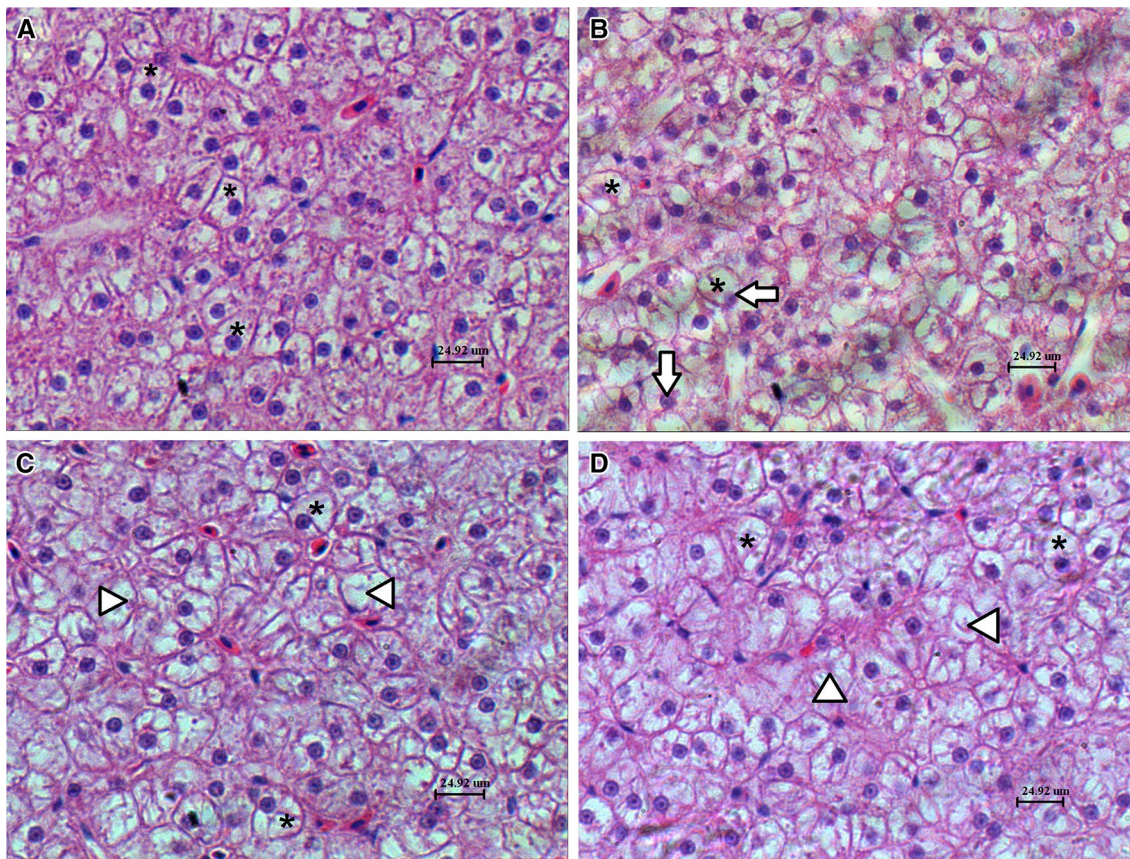


Fig. 1 Representative photographs of hematoxylin-eosin staining histopathological assessment of livers of fish fed four different diets for 56 days: control (a), high-fat (b), high-carbohydrate (c), and high-fat-high-carbohydrate (d) diet. a Small lipid droplets asterisk and large nuclei (visible as a purple spot within each cell); b moderate

lipid droplets asterisk and swelling hepatocytes with irregular nucleus located at the periphery of the cell (arrow); c, d large lipid droplets asterisk, with swollen hepatocytes and nuclear degeneration (head arrow). Scale bar 24.92 μm. (Color figure online)

lipid accumulation observed in livers of human subjects administered high fructose diet (Schwarz et al. 2015), as well as in high-carbohydrate diet-fed fish (*Oreochromis niloticus*), probably as a result of de novo lipid synthesis in liver (Hemre et al. 2002; Shimeno et al. 1993).

3.2 Diet-induced metabolomics changes

¹H NMR-inferred metabolite profiles in plasma and liver extracts from the four groups are shown in supporting information Figure S1. The assignments were further confirmed individually with data from a series of 2D NMR spectra including COSY, TOCSY, JRES, HSQC and HMBC (Fig. S2). ¹H and ¹³C NMR spectra indicated 47 detectable abundant metabolites on the basis of the KEGG database and the available literature data (Allen et al. 2015; An et al. 2013; Duan et al. 2013; Jiang et al. 2013). These included lipoproteins, lipids, organic acids (e.g. TCA intermediates), a variety of amino acids, carbohydrates (e.g. glucose) and microbial metabolism-associated metabolites

(e.g. trimethylamine) (Table S1). In order to infer the comparative metabolomic changes among the four diets, multivariate data analysis was conducted on the OPLS-DA models of plasma and liver extracts. CV-ANOVA analysis of the OPLS-DA model score plots of metabolites indicates significant ($p < 0.05$) differences in metabolites in five out of six group pairs in plasma (control versus HCD, control versus HFHCD, HFD versus HCD, HFD versus HFHCD and HCD versus HFHCD), and two out of six in liver (control vs. HCD and HFD vs. HCD) (Fig. 2). However, as the p values for the control vs. HFD pair in plasma (0.059, Fig. S3) and HFD versus HFHCD pair in liver (0.053, Fig. S4) were barely above the chosen significance threshold (0.05), it can be safely presumed that the differences between these two groups were also substantial. Results of the PLS-DA model score plots and permutation tests (Supplementary data: Fig. S5) indicated good quality of the model, as R^2 and Q^2 values of the real model were always larger than R^2 and Q^2 values from the permutation tests (Eriksson et al. 2008).

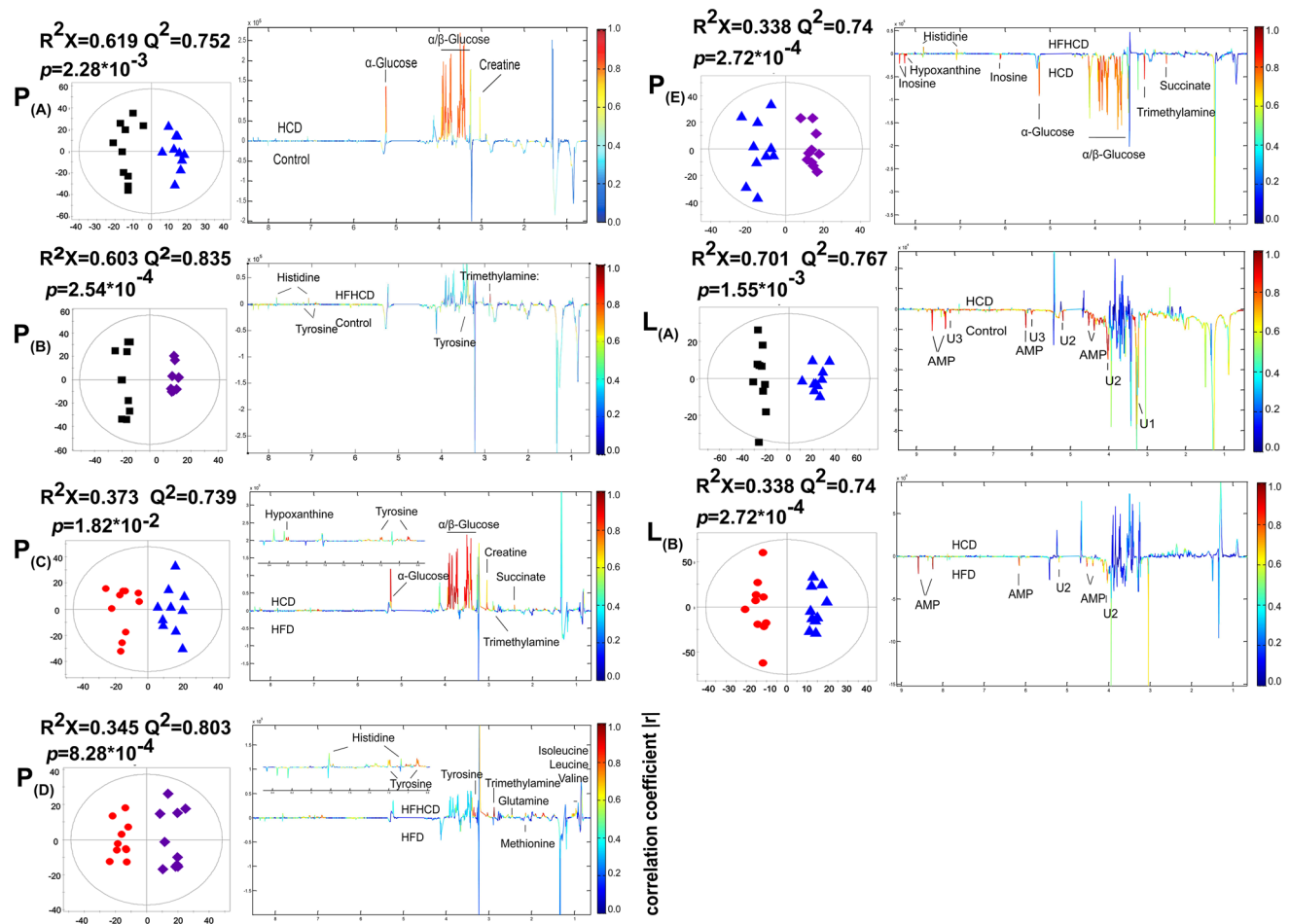


Fig. 2 ^1H NMR data-derived OPLS-DA scores plots (left) and the corresponding loading plots (right). Only the six diet-group pairs with significant differences ($|r| > 0.602$) in metabolite concentrations in plasma (P) and liver (L) are shown. $P_{(A)}$ Control (filled square)

versus HCD (filled triangle), $P_{(B)}$ Control versus HFHCD (filled diamond), $P_{(C)}$ HFD (filled circle) versus HCD, $P_{(D)}$ HF versus HFHCD, $P_{(E)}$ HCD versus HFHCD, $L_{(A)}$ Control versus HCD, $L_{(B)}$ HFD versus HCD

3.3 Specific pathways affected by the high-carbohydrate diet

In comparison to the HFHCD group, α/β -glucose, TMA, inosine, succinate and hypoxanthine levels were significantly higher in plasma of the HCD group, whereas histidine was suppressed (Fig. 2; Table 2). In liver samples, adenosine monophosphate (purine metabolism) and an unknown metabolite were lower in HCD in comparison to HFD (Fig. 2L_(B)). In plasma, apart from inosine, and along with tyrosine and creatine, all those metabolites were also higher in comparison to HFD group. In comparison to the control group, α/β -glucose and creatine were elevated in the HCD group. In liver samples, adenosine monophosphate (purine metabolism) and three unknown metabolites were all lower in the HCD in comparison to control group (Fig. 2L_(A)). None statistically significant ($p > 0.05$) changes were found between control/HFD, control/

HFHCD, HFD/HFHCD and HCD/HFHCD group pairs in liver. The ten known metabolites were associated with the following metabolic processes: glycolysis (α -/ β -glucose), gut microbiota metabolism (TMA), creatine metabolism (creatine), purine metabolism (AMP, inosine and hypoxanthine), histidine metabolism (histidine) and TCA cycle (succinate and tyrosine) (Fig. 2; Table 2).

Energy pathways: glycolysis, TCA cycle and creatine pathway

Three out of these seven metabolites are associated with metabolic pathways involved in energy homeostasis (TCA and glycolysis). High levels of TCA intermediates in association with high carbohydrate diet were also observed in studies on mice (Jung et al. 2012). α - and β -D glucose in glycolysis pathway are metabolized into pyruvate, and then enter the TCA cycle (An et al. 2013), so elevated levels of these two metabolites in the HCD group are probably a reflection of high activity in the glycolysis pathway in

Table 2 Significantly different metabolites between group pairs in plasma (P) and liver (L) extracts, with corresponding correlation coefficients

Metabolic pathway	Metabolites	CD versus HCD ^a	CD versus HFHCD	HFD versus HCD ^a	HFD versus HFHCD	HCD versus HFHCD
Amino acids	Isoleucine (P)				0.74	
	Leucine (P)				0.66	
	Valine (P)				0.73	
	Glutamine (P)				0.77	
One carbon	Methionine (P)				0.72	
Glycolysis	β-Glucose (P)	0.72		0.74		-0.66
	α-Glucose (P)	0.79		0.80		-0.70
TCA cycle	Succinate (P)			0.64		-0.74
	Tyrosine (P)		0.68	0.70	0.67	
Gut microbiota	Trimethylamine (P)	0.57	0.96	0.65	0.98	-0.81
Creatine pathway	Creatine (P)	0.70		0.66		
Histidine	Histidine (P)		0.69		0.64	0.72
Purine	AMP (L)	-0.76		-0.79		
	Inosine (P)	0.22	-0.59	0.48	-0.54	-0.78
	Hypoxanthine (P)		-0.56	0.75		-0.86
Unknown ^b	U1 (L)	-0.71				
	U2 (L)	-0.86		-0.74		
	U3 (L)	-0.69				

Correlation coefficient values indicating significantly different ($|r| > 0.6020$) metabolite levels between pairs of groups are bolded

With left group as the control and right group as the test group, positive values indicate an increase in the amount of metabolite in the test group, whereas negative values indicate a decrease

Blank fields mean that the differences were too small to be reliably measured

CD control diet, HFD high-fat diet, HCD high-carbohydrate diet, HFHCD high-fat-high-carbohydrate diet, AMP adenosine monophosphate

CD\HFD pair is not shown as no significant differences were found ($p > 0.05$)

^aMarks group pairs with significantly different ($p < 0.05$) metabolites in both plasma and liver samples

^bThe available information about the unknown metabolites (U1, U2 and U3) is included in Table S1

comparison to control and HFD diets. Similar observation was made in humans, where high level of dietary glucose has resulted in increased carbohydrate oxidation (Yki-Järvinen et al. 1987). HCD diet also resulted in elevated tyrosine levels in comparison to HFD diet. Tyrosine is a precursor to succinate (via fumarate), which then enters the TCA cycle (Fig. 4). Hence, somewhat predictably, high carbohydrate diet has predominantly affected the metabolites involved in the TCA cycle.

Fish, in contrast to mammals, have limited ability to metabolize glucose for energy purposes, even though they possess the entire enzymatic machinery necessary for carbohydrate utilization. Excess glucose can be stored in liver as glycogen or fatty acids via *de novo* lipogenesis (DNL) (Hemre et al. 2002). Excess energy can also be stored as phosphocreatine, which acts as energy reserve used to regenerate the ATP. Hence, creatine, with its cell energy shuttle function, is a critical component of the maintenance of cellular energy homeostasis (Owen and Sunram-Lea 2011). High creatine levels observed in the HCD-fed

fish could be a metabolic response to energy stress, which could also account for lower growth rates in this group (Wagner et al. 2014). Oxaloacetate (a TCA cycle metabolite) is a precursor for creatine via L-aspartate, arginine and guanidinoacetate (GAA) (Wyss and Daouk 2000). In agreement with the hypothesis of the increased creatine synthesis from the TCA cycle precursors are also the elevated AST levels (the enzyme that catalyzes the first reaction in this chain: oxaloacetate to L-aspartate, which also yields α-ketoglutarate in TCA cycle) in the HCD group (Table 2). GAA is biosynthesized from arginine and glycine in kidney, and then transported to liver, where creatine is biosynthesized via the methylation of GAA by the GAMT enzyme. Creatine is subsequently released into the blood system and transported by blood to the tissues that may require it (Wyss and Daouk 2000). The connection of aspartate and energy metabolism was also observed in an echinoderm, *Apostichopus japonicus*, where aspartate levels significantly decreased after thermal stress, which was associated with the replenishment of a TCA intermediate,

oxaloacetate, as well as the synthesis of α -ketoglutarate via aspartate transamination reactions (Shanware et al. 2011; Shao et al. 2015). Similarly, a decrease of creatinine in creatine pathway in response to a decrease in L-aspartate mammals, have limited zebrafish (Zhao et al. 2014).

3.3.1 Purine metabolism

HCD intake was also associated with the decrease in adenosine monophosphate (AMP) in liver, in comparison to both control ($r = -0.76$) and HFD ($r = -0.79$) groups. A possible explanation is that AMP can be converted to inosine (via IMP), which was elevated in the plasma of HCD group in comparison to both HFD ($r = 0.48$) and control ($r = 0.22$) groups (Table 2). Hypoxanthine was elevated in the plasma of HCD group in comparison to both high fat diets (HFD and HFHCD), but not in comparison to the control group, which indicates that this metabolite decreases in association with high-fat diets. A very similar observation was made for inosine, but it was significantly elevated only in comparison to the HFHCD group (Table 2). This is in very good agreement with the observed high purine catabolism as a result of HFD-induced oxidative stress in rats (An et al. 2013), wherein inosine (a product of nucleotide degradation) is converted into hypoxanthine, which is then further transformed into xanthine (Fig. 4). Xanthine oxidase, which is known to be an indicator of oxidative stress (Erdei et al. 2006), catalyzes further oxidation of hypoxanthine (Fig. 4) (An et al. 2013; Shi et al. 2013). However, as the r values of plasma inosine and hypoxanthine in the HFHCD group were very close to the chosen cut-off value (0.602) in comparison to the control (-0.59 , -0.56 , respectively; Table 2), and only for plasma inosine in comparison to HFD group (-0.54), it can be safely presumed that the differences in these metabolites were substantial between these two groups. These results suggest that the HFHC diet has induced oxidative stress and associated xanthine oxidase activity (Erdei et al. 2006), which has led to reduced inosine and hypoxanthine levels (An et al. 2013).

Heightened energy metabolism associated with high-carbohydrate diet (Horton et al. 1995) appears to have led to an increase of downstream metabolites in purine catabolism, resulting in statistically significant differences between HFD and HCD groups. Elevated levels of hypoxanthine are probably a consequence of disruption of its oxidation into xanthine. As the reaction requires the coenzyme NAD^+ as an oxidizing agent (electron transfer reaction), this could be a consequence of the insufficient supply of NAD^+ (Duan et al. 2013). Another possible explanation for the elevated hypoxanthine levels could be the up-regulation of purine-nucleoside phosphorylase (which converts inosine to hypoxanthine) in association

with HCD observed in other experiments in our lab (transcriptome analysis, unpublished data).

3.3.2 Specific pathways affected by the HFHC diet

Among the eight metabolites significantly elevated in the HFHCD group, TMA (gut microbiota metabolism) and histidine (AA) were shared among all three group-pairs (HFHCD/control, /HFD and /HCD) (Table 2). Apart from these two metabolites, HFHCD/control and HFHCD/HFD group pairs also shared tyrosine (AA). The five metabolites significantly elevated only in comparison to the HFD group were also all amino acids: isoleucine, leucine, valine, glutamine (amino acids metabolism) and methionine (one-carbon metabolism) (Table 2). In liver samples, there were no statistically significant changes in control versus HFHCD, HFD versus HFHCD and HCD versus HFHCD group-pairs ($p > 0.05$).

3.3.3 Amino acids metabolism

Hence, HFHCD intake caused a significant increase in seven different AAs. Three of these (leucine, isoleucine and valine) were branched-chain AAs (BCAAs), which are among the nine essential amino acids. BCAAs can contribute to the energy metabolism by expanding the pool of TCA cycle intermediates (anaplerosis) (Wagner et al. 2014) and entering the gluconeogenesis (Shimomura et al. 2004). The remaining four, glutamine, histidine, methionine and tyrosine, can also contribute to the TCA cycle (Figs. 3, 4). Via glutamate, glutamine is as a precursor of an intermediate in the TCA cycle, α -ketoglutarate, (Shanware et al. 2011; Yelamanchi et al. 2016). Glutamate is also an important precursor in the amino acids metabolism, as well as a product of histidine catabolism, which is the only metabolite that was consistently (in all pairwise group comparisons) induced by (and only by) the HCHFD (Table 2; Fig. 4). As AAs normally enter the TCA cycle (via the TCA cycle intermediates) and gluconeogenesis (via acetyl CoA and pyruvate) only in the absence of a sufficient amount of dietary carbohydrates, high concentration of these seven amino acids in the plasma of fish fed HFHC diet could be a consequence of the "congestion" of TCA cycle as a result of the excess of the products of carbohydrate and lipid metabolisms, leading to significantly reduced numbers of amino acids entering the cycle (Bunthawiyuwat 2003). However, the excess of five of these amino acids (BCAAs, glutamine and methionine) in the HFHCD group only in comparison to HFD group is intriguing, as they did not appear to be significantly different in the remaining two HFHCD pairs (.../HCD and .../control) (Table 2). This implies that the concentration of these five amino acids was lower in the plasma of the HFD group in comparison

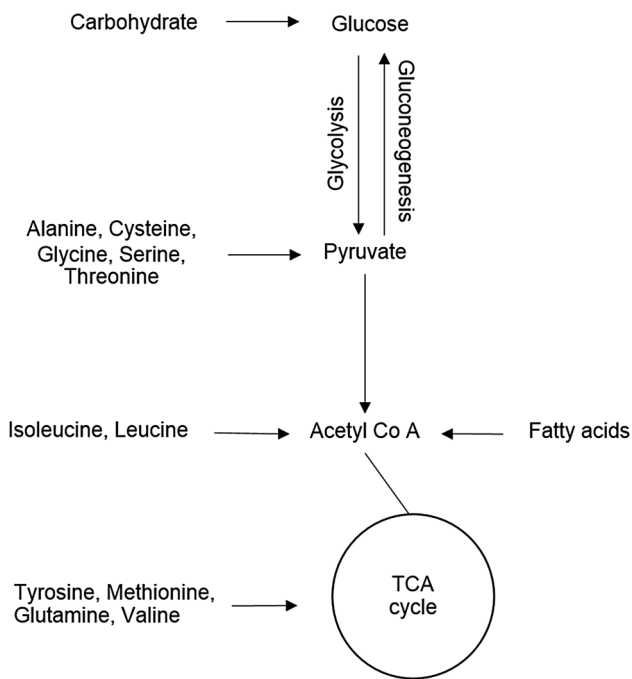


Fig. 3 Relationships among the metabolic pathways of glucose, amino acids and fatty acids

to HCD and control diet groups, which was also observed in high-fat diet fed rats (An et al. 2013; Xie et al. 2010). A possible explanation could be that a small ratio of carbohydrates in the high-fat diet has resulted in amino acids being used for gluconeogenesis (via pyruvate) (An et al. 2013). This hypothesis is further supported by the elevated glutamine level in the HFHCD group, as it is in agreement with the observation that glutamine levels increase together with the LDL levels in atherosclerosis (An et al. 2013).

3.3.4 Histidine and one-carbon metabolism

It should be noted that these amino acids partake in other metabolic pathways as well, which can also influence their levels. Histidine is a precursor to histamine, which can accelerate lipolysis (Kim et al. 2010; Yoshimatsu et al. 2002). Methionine, which was elevated in the HFHCD in comparison to HFD, plays an important role in the one-carbon metabolism. Methionine production is essential for most biological methylation reactions that use S-adenosyl-methionine (SAM) as the methyl donor (Lever and Slow 2010). As high homocysteine and low SAM levels have been associated with some chronic coronary (atherosclerosis) and hepatic (nonalcoholic fatty liver) diseases (Jiang et al. 2013; Peng et al. 2011; Xie et al. 2010), increased levels of plasma methionine could be also a consequence of

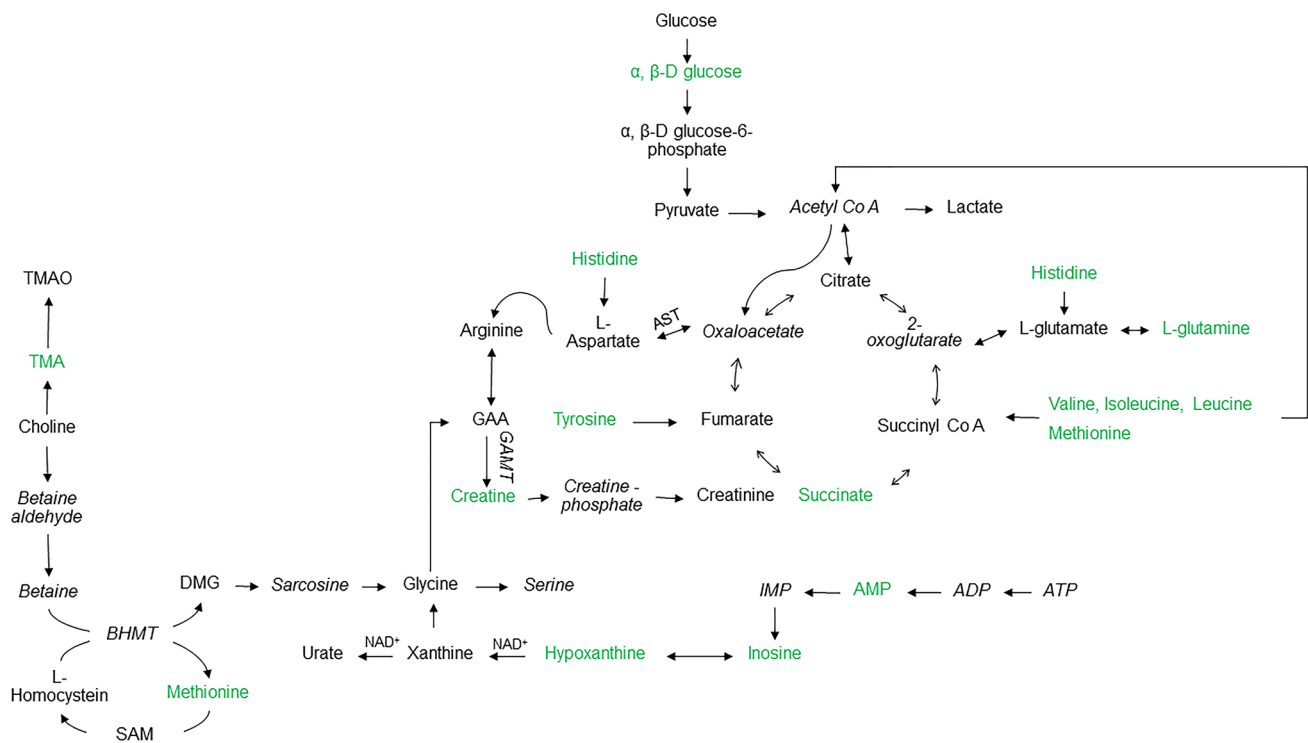


Fig. 4 High-fat-high-carbohydrate diet-induced changes in metabolic pathways. Metabolites in green were significantly changed. Metabolites in non-italicized black font did not show significant differences,

whereas *italicized font* indicates the metabolite was not measured. (Color figure online)

an inbuilt self-protection mechanism, wherein homocysteine is rapidly re-methylated to methionine by the BHMT enzyme (Fig. 4). This conversion could also lead to low SAM concentrations. It is known that a high-methionine diet induces atherosclerosis in rabbits. Disturbances in lipid peroxidation and antioxidant activities are a possible mechanism of its atherogenic influence (Toborek et al. 1995). Atherosclerosis begins with damage to the endothelium of arteries caused by the LDL (so-called “bad cholesterol”). High methionine levels in plasma lead to enhanced uptake and synthesis of cholesterol by the liver and its release into the blood in the form of LDL (Lever and Slow 2010). High plasma levels of LDL cholesterol observed in the HFHCD group (Table 1) are in agreement with this scenario.

3.4 Metabolic pathways affected by both HCD and HFHCD diets

3.4.1 Energy pathways

HFHCD induced tyrosine elevation in comparison to the control and HFD groups, whereas there were no significant differences in comparison to the HCD group. Tyrosine was also significantly elevated by the HCD in comparison to HFD, but not in comparison to the control group. In mice, elevated tyrosine levels were also associated with HCD, but not with HFD (Jung et al. 2012). This further indicates “congestion” of the TCA cycle as a result of the excess of carbohydrates, leading to a significantly reduced amount of tyrosine entering the cycle (Bunthawiyuwat 2003) (Figs. 3, 4). Similarly, in humans, high-fructose diet can suppress gluconeogenesis, resulting in the products of carbohydrate and fat metabolism directly entering the TCA cycle (Schwarz et al. 2015).

3.4.2 Gut microbiota metabolism.

Trimethylamine (TMA, a byproduct of the gut microbiota metabolism) levels were also elevated in both high-carbohydrate diet groups (HCD and HFHCD; Table 2). TMA is a gaseous product of the bacterial metabolism in guts (Al-Waiz et al. 1992), which is then absorbed and metabolized in liver to trimethylamine-N-oxide (TMAO; Fig. 4) (Wang et al. 2011). TMAO was found in high levels in some freshwater fish, such as tilapia and Nile perch (*Lates niloticus*) (Anthoni et al. 1990). Our results support a previous finding (Li et al. 2016) that the activity of gut microbiota is in a strong positive correlation with the amount of carbohydrates in diet. As both HC diets (HCD and HFHCD) exhibited elevated TMA levels in comparison to the HFD, and as TMA levels were also significantly induced by the HCD in comparison to the HFHCD, this indicates that high fat content in a diet has interfered with the TMA production by

gut microbiota. This is in agreement with the decrease in total gut bacteria levels associated with HFD diet-induced obesity observed previously in mice (Jung et al. 2012; Kim et al. 2010). In animal models (Dumas et al. 2006), as well as in humans (Spencer et al. 2011), gastrointestinal microbes (GI) can disrupt the bioavailability of choline to the host by converting choline to methylamine, thus causing the development of non-alcoholic fatty liver disease. However, the same GI microbes that are believed to cause choline deficiency in mammals have been reported as dominant microbiota in another herbivorous fish, grass carp, fed high cellulose diet (Ni et al. 2014). Somewhat inconsistently, in comparison to the control, TMA levels were only significantly elevated by the HFHCD, and not by HCD. However, as the *r* value for this metabolite (0.57) between control and HCD groups was very close to the selected cut-off value (0.602), it can be safely presumed that differences in the levels of this metabolite between these two groups were also substantial (Table 2).

4 Conclusions

The excess energy availability in the fish fed high-carbohydrate diet has led to increased levels of a number of metabolites in the central metabolic energy pathway and elevated creatine levels. High-fat-high-carbohydrate diet appears to have led to the “congestion” of the TCA cycle, elevated a number of amino acids. This excess energy has then caused further elevation in metabolites associated with one-carbon metabolism through high re-methylation, eventually leading to oxidative stress. Clinical chemistry and histological analyses also support this conclusion. Hence, the results of our study indicate that in *M. amblycephala* high carbohydrate diet leads to a disruption of the TCA cycle and energy homeostasis, and generally causes much stronger metabolic disturbances than high fat diet. Furthermore, in comparison to HFD, high carbohydrate diets also caused stronger signs of liver damage and high levels of LDL, which can be a predictor of several chronic diseases. Finally, high fat diets resulted in higher average final weight in comparison to HCD. This indicates that *M. amblycephala* is very efficient in metabolizing fatty acids, both for producing the energy via acetyl CoA entering the central metabolic energy pathway and for directly storing it in fat deposits as energy reserve. However, similar to humans (Hellerstein 1999), it appears to be less efficient in *de novo* lipogenesis, resulting in lower final weight. Unsurprisingly (Ni et al. 2014), there was a strong positive correlation between the gut microbiota metabolism and the amount of carbohydrates in the diet. Hence, it would be interesting to test in future studies whether high TMA production by gut microbiota can also disrupt the bioavailability of choline and cause

the development of non-alcoholic fatty liver disease in *M. amblycephala*. Regardless, these results confirm the suitability of metabolomics for studying diet-induced metabolic disorders that often lead to substantial financial losses in the aquaculture of *M. amblycephala*. A thorough understanding of these metabolic changes is an important step towards understanding the progression of diseases caused by dietary imbalances.

Acknowledgements This study was supported by Natural Science Foundation of China (No. 31401976), the earmarked fund for the Fundamental Research Funds for the Central Universities (2662015PY019) and Modern Agro-industry Technology Research System entitled “Staple Freshwater Fishery Industry Technology System” (No. CARS-46-05).

Compliance with ethical standards

Conflict of interest The authors have declared that no conflict of interest exists.

Ethical approval All applicable international, national and/or institutional guidelines for the care and use of animals were followed.

References

- Akhtar, M. T., Mushtaq, M. Y., Verpoorte, R., Richardson, M. K., & Choi, Y. H. (2016). Metabolic effects of cannabinoids in zebrafish (*Danio rerio*) embryos determined by ¹H NMR metabolomics. *Metabolomics*, 12(3), 1–11. doi:10.1007/s11306-016-0964-2.
- Allen, P. J., Wise, D., Greenway, T., Khoo, L., Griffin, M. J., & Jablonsky, M. (2015). Using 1-D 1 H and 2-D 1 H J-resolved NMR metabolomics to understand the effects of anemia in channel catfish (*Ictalurus punctatus*). *Metabolomics*, 11(5), 1131–1143. doi:10.1007/s11306-014-0767-2.
- Al-Waiz, M., Mikov, M., Mitchell, S. C., & Smith, R. L. (1992). The exogenous origin of trimethylamine in the mouse. *Metabolism*, 41, 135–136.
- An, Y., Xu, W., Li, H., Lei, H., Zhang, L., Hao, F., et al. (2013). High-fat diet induces dynamic metabolic alterations in multiple biological matrices of rats. *Journal of Proteome Research*, 12(8), 3755–3768. doi:10.1021/pr400398b.
- Anthoni, U., Børresen, T., Christophersen, C., Gram, L., & Nielsen, P. H. (1990). Is trimethylamine oxide a reliable indicator for the marine origin of fish. *Comparative Biochemistry and Physiology Part B*, 97(3), 569–571. doi:10.1016/0305-0491(90)90161-L.
- Asai, A., Chou, P. M., Bu, H.-F., Wang, X., Rao, M. S., Jiang, A., et al. (2014). Dissociation of hepatic insulin resistance from susceptibility of nonalcoholic fatty liver disease induced by a high-fat and high-carbohydrate diet in mice. *American Journal of Physiology-Gastrointestinal and Liver Physiology*, 306(6), G496–G504. doi:10.1152/ajpgi.00291.2013.
- Bunthawiyuwat, N. (2003). Energy Metabolism. In *Nutritional biochemistry* (pp. 179–180). Bangkok: Sigma Design Graphic.
- Dai, H., Xiao, C., Liu, H., Hao, F., & Tang, H. (2010). Combined NMR and LC-DAD-MS analysis reveals comprehensive metabonomic variations for three phenotypic cultivars of salvia miltiorrhiza bunge. *Journal of Proteome Research*, 9(3), 1565–1578. doi:10.1021/pr901045c.
- Dai, H., Xiao, C., Liu, H., & Tang, H. (2010). Combined NMR and LC-MS analysis reveals the metabonomic changes in salvia miltiorrhiza bunge induced by water depletion. *Journal of Proteome Research*, 9(3), 1460–1475. doi:10.1021/pr900995m.
- Duan, Y., An, Y., Li, N., Liu, B., Wang, Y., & Tang, H. (2013). Multiple univariate data analysis reveals the inulin effects on the high-fat-diet induced metabolic alterations in rat myocardium and testicles in the preobesity state. *J Proteome Research*, 12(7), 3480–3495. doi:10.1021/pr400341f.
- Dumas, M. E., Barton, R. H., Toye, A., Cloarec, O., Blancher, C., Rothwell, A., et al. (2006). Metabolic profiling reveals a contribution of gut microbiota to fatty liver phenotype in insulin-resistant mice. *Proceedings of the National Academy of Sciences*, 103(33), 12511–12516. doi:10.1073/pnas.0601056103.
- Dunn, W. B., Broadhurst, D. I., Atherton, H. J., Goodacre, R., & Griffin, J. L. (2011). Systems level studies of mammalian metabolomes: the roles of mass spectrometry and nuclear magnetic resonance spectroscopy. *Chemical Society Reviews*, 40(1), 387–426. doi:10.1039/b906712b.
- Erdei, N., Toth, A., Pasztor, E. T., Papp, Z., Edes, I., Koller, A., & Bagi, Z. (2006). High-fat diet-induced reduction in nitric oxide-dependent arteriolar dilation in rats: Role of xanthine oxidase-derived superoxide anion. *American Journal of Physiology-Heart and Circulatory Physiology*, 291, 2107–2115.
- Eriksson, L., Trygg, J., & Wold, S. (2008). CV-ANOVA for significance testing of PLS and OPLS[®] models. *Journal of Chemometrics*, 22(11–12), 594–600. doi:10.1002/cem.1187.
- Figueiredo-Silva, A. C., Panserat, S., Kaushik, S., Geurden, I., & Polakof, S. (2012). High levels of dietary fat impair glucose homeostasis in rainbow trout. *Journal of Experimental Biology*, 215(Pt 1), 169–178. doi:10.1242/jeb.063933.
- Food and Agriculture Organization of the United Nations. (2013). FAO statistical yearbook 2013[†]: World food and agriculture.
- Gao, W., Liu, Y. J., Tian, L. X., Mai, K. S., Liang, G. Y., Yang, H. J., et al. (2009). Effect of dietary carbohydrate-to-lipid ratios on growth performance, body composition, nutrient utilization and hepatic enzymes activities of herbivorous grass carp (*Ctenopharyngodon idella*). *Aquaculture Nutrition*, 16(3), 327–333. doi:10.1111/j.1365-2095.2009.00668.x.
- Ge, C. X., Yu, R., Xu, M. X., Li, P. Q., Fan, C. Y., Li, J. M., & Kong, L. D. (2016). Betaine prevented fructose-induced NAFLD by regulating LX α /PPAR α pathway and alleviating ER stress in rats. *European Journal of Pharmacology*, 770, 154–164. doi:10.1016/j.ejphar.2015.11.043.
- Hellerstein, M. K. (1999). De novo lipogenesis in humans: metabolic and regulatory aspects. *European Journal of Clinical Nutrition*, 53(s1), S53–65. doi:10.1038/SJ.EJCN.1600744.
- Hemre, G. I., Mommsen, T. P., & Krogdahl, Å (2002). Carbohydrates in fish nutrition: Effects on growth, glucose metabolism and hepatic enzymes. *Aquaculture Nutrition*, 8(3), 175–194. doi:10.1046/j.1365-2095.2002.00200.x.
- Horton, T. J., Drougas, H., Brachey, A., Reed, G. W., Peters, J. C., & Hill, J. O. (1995). Fat and carbohydrate overfeeding in humans: different effects on energy storage. *The American Journal of Clinical Nutrition*, 62, 19–29.
- Jiang, Y., Yang, M., Yang, L., Miao, X., Wang, H., & Zhu, B. (2013). A ¹H NMR-BASED metabonomic investigation of time-related metabolic trajectories of the plasma, urine and liver extracts of hyperlipidemic hamsters. *PLoS One*, 8, E66786. doi:10.1371/journal.pone.0066786.t001
- Jung, J. Y., Kim, I. Y., Kim, Y. N., Kim, J. S., Shin, J. H., Jang, Z. H., et al. (2012). ¹H NMR-based metabolite profiling of diet-induced obesity in a mouse model. *BMB Reports*, 45(7), 419–424. doi:10.5483/BMBRep.2012.45.7.248.
- Kim, I. Y., Jung, J., Jang, M., Ahn, Y. G., Shin, J. H., Choi, J. W., et al. (2010). ¹H NMR-based metabolomic study on resistance

- to diet-induced obesity in AHNAK knock-out mice. *Biochemical and Biophysical Research Communications*, 403(3–4), 428–434. doi:10.1016/j.bbrc.2010.11.048.
- Koteish, A., & Diehl, A. M. (2001). Animal models of steatosis. *Seminars in Liver Disease*, 21(1), 89–104. doi:10.1055/s-2001-12932.
- Kullgren, A., Samuelsson, L. M., Larsson, D. G., Bjornsson, B. T., & Bergman, E. J. (2010). A metabolomics approach to elucidate effects of food deprivation in juvenile rainbow trout (*Oncorhynchus mykiss*). *American Journal of Physiology-Regulatory, Integrative and Comparative Physiology*, 299(6), R1440–R1448. doi:10.1152/ajpregu.00281.2010.
- Lever, M., & Slow, S. (2010). The clinical significance of betaine, an osmolyte with a key role in methyl group metabolism. *Clinical Biochemistry*, 43(9), 732–744. doi:10.1016/j.clinbiochem.2010.03.009.
- Li, H., Wu, S., Wirth, S., Hao, Y., Wang, W., Zou, H., et al. (2016). Diversity and activity of cellulolytic bacteria, isolated from the gut contents of grass carp (*Ctenopharyngodon idellus*) (Valenciennes) fed on Sudan grass (*Sorghum sudanense*) or artificial feedstuffs. *Aquaculture Research*, 47(1), 153–164. doi:10.1111/are.12478.
- Li, X. F., Liu, W. B., Lu, K. L., Xu, W. N., & Wang, Y. (2012). Dietary carbohydrate/lipid ratios affect stress, oxidative status and non-specific immune responses of fingerling blunt snout bream, *Megalobrama amblycephala*. *Fish Shellfish Immunol*, 33(2), 316–323. Journal Article. doi:10.1016/j.fsi.2012.05.007.
- Li, X. F., Lu, K. L., Liu, W. B., Jiang, G. Z., & Xu, W. N. (2014). Effects of dietary lipid and carbohydrate and their interaction on growth performance and body composition of Juvenile Blunt Snout Bream, *Megalobrama amblycephala*. *The Israeli Journal of Aquaculture - Bamiddeh*, 66, 1–7.
- Li, X. F., Wang, Y., Liu, W. B., Jiang, G. Z., & Zhu, J. (2013). Effects of dietary carbohydrate/lipid ratios on growth performance, body composition and glucose metabolism of fingerling blunt snout bream *Megalobrama amblycephala*. *Aquaculture Nutrition*, 19(5), 701–708. doi:10.1111/anu.12017.
- Ni, J., Yan, Q., Yu, Y., & Zhang, T. (2014). Factors influencing the grass carp gut microbiome and its effect on metabolism. *FEMS Microbiology Ecology*, 87(3).
- Ong, E. S., Chor, C. F., Zou, L., & Ong, C. N. (2009). A multi-analytical approach for metabolomic profiling of zebrafish (*Danio rerio*) livers. *Molecular bioSystems*, 5(3), 288–298. doi:10.1039/b811850g.
- Owen, L., & Sunram-Lea, S. I. (2011). Metabolic agents that enhance ATP can improve cognitive functioning: A review of the evidence for glucose, oxygen, pyruvate, creatine, and L-carnitine. *Nutrients*. doi:10.3390/nu3080735.
- Peng, J. B., Jia, H. M., Xu, T., Liu, Y. T., Zhang, H. W., Yu, L. L., et al. (2011). A ¹H NMR based metabolomics approach to progression of coronary atherosclerosis in a rabbit model. *Process Biochemistry* (Oxford, U. K.), 46(12), 2240–2247. doi:10.1016/j.procbio.2011.08.016.
- Polakof, S., Medale, F., Larroquet, L., Vachot, C., Corraze, G., & Panserat, S. (2011). Regulation of de novo hepatic lipogenesis by insulin infusion in rainbow trout fed a high-carbohydrate diet. *J. Anim. Sci.*, 89(10), 3079–3088. doi:10.2527/jas.2010-3733.
- Qiu, L., Song, Q., Jiang, X., Zhao, H., Chen, H., Zhou, H., et al. (2016). Comparative gonad protein and metabolite responses to a binary mixture of 2,4'-DDT and benzo(a)pyrene in the female green mussel *Perna viridis*. *Metabolomics*, 12(8), 140. doi:10.1007/s11306-016-1089-3.
- Ren, M., Habte-Tsion, H. M., Xie, J., Liu, B., Zhou, Q., Ge, X., et al. (2015). Effects of dietary carbohydrate source on growth performance, diet digestibility and liver glucose enzyme activity in blunt snout bream, *Megalobrama amblycephala*. *Aquaculture*, 438, 75–81. doi:10.1016/j.aquaculture.2015.01.008.
- Schock, T. B., Newton, S., Brenkert, K., Leffler, J., & Bearden, D. W. (2012). An NMR-based metabolomic assessment of cultured cobia health in response to dietary manipulation. *Food Chem.*, 133(1), 90–101. doi:10.1016/j.foodchem.2011.12.077.
- Schwarz, J. M., Noworolski, S. M., Wen, M. J., Dyachenko, A., Prior, J. L., Weinberg, M. E., et al. (2015). Effect of a high-fructose weight-maintaining diet on lipogenesis and liver fat. *Journal of Clinical Endocrinology and Metabolism*, 100(6), 2434–2442. doi:10.1210/jc.2014-3678.
- Shanware, N. P., Mullen, A. R., DeBerardinis, R. J., & Abraham, R. T. (2011). Glutamine: Pleiotropic roles in tumor growth and stress resistance. *Journal of Molecular Medicine*. doi:10.1007/s00109-011-0731-9.
- Shao, Y., Li, C., Chen, X., Zhang, P., Li, Y., Li, T., & Jiang, J. (2015). Metabolomic responses of sea cucumber *Apostichopus japonicus* to thermal stresses. *Aquaculture*. doi:10.1016/j.aquaculture.2014.10.023.
- Shi, X., Xiao, C., Wang, Y., & Tang, H. (2013). Gallic acid intake induces alterations to systems metabolism in rats. *Journal of Proteome Research*, 12(2), 991–1006. doi:10.1021/pr301041k.
- Shimeno, S., Ming, D.-C., & Takeda, M. (1993). Metabolic response to dietary carbohydrate to lipid ratios in *Oreochromis niloticus*. *NIPPON SUISAN GAKKAISHI*, 59(5), 827–833. doi:10.2331/suisan.59.827.
- Shimomura, Y., Murakami, T., Nakai, N., Nagasaki, M., & Harris, R. A. (2004). Exercise promotes BCAA catabolism: Effects of BCAA supplementation on skeletal muscle during exercise. *The Journal of Nutrition*, 134(6), 1583S–1587.
- Spencer, M. D., Hamp, T. J., Reid, R. W., Fischer, L. M., Zeisel, S. H., & Fodor, A. A. (2011). Association between composition of the human gastrointestinal microbiome and development of fatty liver with choline deficiency. *Gastroenterology*, 140(3), 976–986. doi:10.1053/j.gastro.2010.11.049.
- Toborek, M., Kopieczna-Grzebieniak, E., Marian Drózd, M., & Wiczorek, M. (1995). Increased lipid peroxidation as a mechanism of methionine-induced atherosclerosis in rabbits. *Atherosclerosis*, 115(2), 217–224. doi:10.1016/0021-9150(94)05516-L.
- Wagner, L., Trattner, S., Pickova, J., Gómez-Requeni, P., & Moazzami, A. A. (2014). ¹H NMR-based metabolomics studies on the effect of sesamin in Atlantic salmon (*Salmo salar*). *Food Chemistry*, 147, 98–105. doi:10.1016/j.foodchem.2013.09.128.
- Wang, X. D., Li, E. C., Wang, S. F., Qin, J. G., Chen, X. F., Lai, Q. M., et al. (2015). Protein-sparing effect of carbohydrate in the diet of white shrimp *Litopenaeus vannamei* at low salinity. *Aquaculture Nutrition*, 21(6), 904–912. doi:10.1111/anu.12221.
- Wang, Z., Klipfell, E., Bennett, B. J., Koeth, R., Levison, B. S., Dugar, B., et al. (2011). Gut flora metabolism of phosphatidylcholine promotes cardiovascular disease. *Nature*, 472(7341), 57–63. doi:10.1038/nature09922.
- Wyss, M., & Daouk, R. K. (2000). Creatine and creatinine metabolism. *Physiological Reviews*, 80(3), 1107–1213.
- Xie, Z., Li, H., Wang, K., Lin, J., Wang, Q., Zhao, G., et al. (2010). Analysis of transcriptome and metabolome profiles alterations in fatty liver induced by high-fat diet in rat. *Metabolism*, 59(4), 554–560. doi:10.1016/j.metabol.2009.08.022.
- Yamashita, H., Takenoshita, M., Sakurai, M., Bruck, R. K., Henzel, W. J., Shillinglaw, W., et al. (2001). A glucose-responsive transcription factor that regulates carbohydrate metabolism in the liver. *Proceedings of the National Academy of Sciences of the United States of America*, 98(16), 9116–9121. doi:10.1073/pnas.161284298.
- Yelamanchi, S. D., Jayaram, S., Thomas, J. K., Gundimeda, S., Khan, A. A., Singhal, A., et al. (2016). A pathway map of glutamate metabolism. *Journal of Cell Communication and Signaling*, 10(1), 69–75. doi:10.1007/s12079-015-0315-5.

- Yki-Järvinen, H., Bogardus, C., & Howard, B. V. (1987). Hyperglycemia stimulates carbohydrate oxidation in humans. *The American Journal of Physiology*, *253*(4 Pt 1), E376–E382.
- Yoshimatsu, H., Tsuda, K., Nijima, A., Tatsukawa, M., Chiba, S., & Sakata, T. (2002). Histidine induces lipolysis through sympathetic nerve in white adipose tissue. *European Journal of Clinical Investigation*, *32*, 236–241.
- Zhao, X., Wu, C., Peng, X., & Li, H. (2014). Interferon- α 2b against microbes through promoting biosynthesis of unsaturated fatty acids. *Journal of Proteome Research*, *13*(9), 4155–4163. doi:[10.1021/pr500592x](https://doi.org/10.1021/pr500592x).
- Zhou, C. P., Ge, X. P., Liu, B., Xie, J., & Miao, L. H. (2013). Effect of high dietary carbohydrate on the growth performance and physiological responses of juvenile wuchang bream, *Megalobrama amblycephala*. *Asian-Australasian Journal of Animal Sciences*, *26*(11), 1598–1608. doi:[10.5713/ajas.2012.12659](https://doi.org/10.5713/ajas.2012.12659).